Spatial and Temporal Dynamics of Two Interacting Modes in Parametrically Driven Surface Waves

H. Arbell and J. Fineberg

The Racah Institute of Physics, The Hebrew University of Jerusalem, Jerusalem 91904, Israel

(Received 23 June 1998)

Nonlinear waves with basic wave numbers, k_1 and k_2, are simultaneously excited via two-frequency parametric excitation of a fluid surface. Three new multiwave states are observed: (1) A superlattice state composed of k_1 and k_2 whose relative orientation is governed by a temporal resonance condition, (2) a superlattice built entirely of wave numbers k_1 and $k_1/2$, and (3) a state composed of wave numbers of lengths k_1 and k_2 that are uncorrelated in both space and time. The three states exhibit interesting temporal as well as spatial behavior and are observed in a variety of frequency combinations. [S0031-9007(98)07620-0]

PACS numbers: 47.54.+r, 47.20.Gv, 47.35.+i, 47.52.+j

Since the discovery that complex behavior in space and time can arise in a controlled deterministic system, both the mechanisms that create disorder and their characterization have captured the interest of physicists. Until recently, most studies of disorder in driven dissipative systems have concentrated on the limiting cases of either pattern-forming systems where a single spatial mode is excited or on the case where a system is highly turbulent and many spatial and temporal degrees of freedom are excited concurrently. In the single mode case, the underlying spatial behavior of the system is dictated by the excited mode and complexity in the system evolves as a result of its secondary instabilities. Well-known examples of such systems are Rayleigh-Benard convection, Couette-Taylor flow, electroconvection, and the Faraday instability. The intermediate case, where a system is unstable to a *finite* number of nonlinearly interacting spatial and temporal modes, has not been widely studied. In this paper we take a step in this direction by the experimental study of a system in which two different unstable modes are externally excited. We will show that qualitatively new spatial and temporal behavior occurs in the near vicinity of the instability onset as nonlinear superlattice-type phases arise. The existence of these states points to a large class of previously unanticipated spatial and temporal states that may prove to be of general significance in nonlinear systems where multiple interacting spatial modes are excited.

A convenient experimental system with which to study interacting spatial modes is that of parametrically driven surface waves. As first noted by Faraday, sinusoidal acceleration of a fluid layer with angular frequency ω in the direction of gravity induces a pattern, having a wave number k, on the fluid surface. Nonlinear wave interactions can be studied in this system by driving the fluid layer at two commensurate frequencies, $\omega_1 = n\omega_0$ and $\omega_2 = m\omega_0$ where n and m are relatively prime integers. We will always assume that $\omega_2 > \omega_1$. The general form of the excitation acceleration function is

$$A[\cos(\chi)\cos(\omega_1 t) + \sin(\chi)\cos(\omega_2 t + \phi)], \quad (1)$$

where the angle, χ, describes the degree of mixing between the two modes. The first to apply two-frequency excitation to surface waves were Edwards and Fauve [1] who observed a quasicrystalline pattern having 12-fold symmetry in k space in a narrow range of ϕ near the system's bicritical point. Linear stability analysis of this system was later performed by Besson *et al.* [2] by extension of the Kumar and Tuckerman [3] analysis for single-frequency forcing. Their predictions for the critical acceleration, a_c, were verified for a number of different fluid viscosities and driving frequency combinations [1,2]. Additional experiments using two-frequency excitations were performed by Muller [4] who showed that for a fixed frequency ratio of $\omega_2/\omega_1 = 2$ triangular patterns could be stabilized relative to hexagonal patterns by the addition of a small third frequency component. Using a two-mode approximation to a Mathieu-type equation, Zhang and Vinals [5] derived an amplitude equation description whose phase diagram qualitatively agrees with these experiments. Lifshitz and Petrich [6] also obtained stable two-frequency states having 2-, 4-, 6-, and 12-fold symmetries, as observed in [1], together with two wave number nonsymmetric states by modeling two interacting waves with a generalized Swift-Hohenberg equation.

Our experiments are performed using Dow-Corning 200 silicone oil with a kinematic viscosity of $\nu = 23$ cS (centistoke). Using the apparatus described in [7], we conducted our experiments in thin fluid layers of height 0.155 cm so as to both reduce effects of lateral boundary enforced quantization and to damp out long wavelength modes. Our fluid cells are circular with a 14.4 cm diameter and constructed of black-anodized aluminum machined to 10 μm flatness. The ω_1/ω_2 combinations used in our experiments were (in Hz) 30/40, 30/50, 30/55, 30/70, 40/50, 40/60, 40/70, 41/60, 45/60, 50/60, 50/70, 50/75, 50/80, 30/70, 40/70, 50/70, and 50/80. Most of our detailed experiments were performed with $\phi = 0$, but no qualitative variation of our results

 0031-9007/98/81(20)/4384(4)$15.00

was observed when ϕ was varied. The temperature of the working fluid was regulated via attached thin-film heaters to 30 ± 0.05 °C.

To visualize the fluid surface, we employed a novel imaging technique. A cylindrical screen, concentric with the experimental cell, upon which light intensity was varied as a function of the height above the fluid, provided illumination. A CCD camera was mounted on the cylinder axis. At each point on the fluid surface, the local slope reflects only a single point from the cylinder surface onto the CCD. Since the lighting provides a unique intensity at each height along the cylinder, the intensity reflected by each point is uniquely mapped to the projection of its slope in the direction of the cylinder axis. The CCD, mounted 1.4 m above the fluid, was computer triggered, thereby enabling us to photograph distinct phases of the moving pattern. A typical two-frequency phase diagram is presented in Fig. 1. Together with square and hexagonal phases, seen in previous experiments, we observe three new states, spatially subharmonic superlattices (SSS) [8], two-mode superlattices (2MS) [8], and spatially and temporally unlocked states ("unlocked" states).

Subharmonic superlattice states occur over a wide range of χ in the two-frequency phase diagram where the lower frequency, ω_1, is dominant. SSS were observed for all odd-odd and even-odd frequency ratios tested, but were *not* seen for odd-even ratios. As Fig. 1 indicates, these states can occur for ω_2 amplitudes far below the single-frequency threshold for k_2 states. The transition to these states from the primary hexagonal instability is (within $\approx 1\%$) nonhysteretic and occurs via propagating fronts. In Fig. 2a we present a sequence of SSS states taken at different times for constant values of the driving parameters. Although the state's appearance changes with time, spatial Fourier spectra reveal that the state results from the interaction of two specific spatial scales; a wave number k_1 corresponding to the parametric frequency ω_1, and its spatial subharmonic, $k_1/2$. The SSS spectra show that while the k_1 wave vector has a 6-fold symmetry, the $k_1/2$ wave vector has broken this symmetry (i.e., consisting of hexagons with "missing" wave vectors as seen in the right panel of Fig. 2a).

This results in the stripes seen in Fig. 2a. The SSS states exhibit spatial phase locking; at a given temporal phase the *locations* of the spectral peaks are fixed, although their relative amplitudes (hence their appearance) will vary. Wave numbers, k_2, corresponding to ω_2, are notably absent in the SSS spectra. The presence of ω_2, however, is reflected in the state's time dependence. As observed in [1,2], the basic frequency of the hexagonal instability preceding the SSS state is either ω_0 or $\omega_0/2$ depending on whether ω_1 is an even or odd multiple of ω_0. Upon transition to SSS states, temporal period doubling relative to the primary instability occurs for most states. (The even-odd states 30/55, 40/50, 40/60, 40/70, and 50/75 Hz have a basic frequency of $\omega_0/2$, whereas the odd-odd ratios 30/70 and 50/70 Hz have a fundamental $\omega_0/4$ frequency.) For other frequency ratios the state's underlying time dependence is more complex. Upon increase of the ω_1 amplitude, the SSS become unstable to slow temporal "breathing" modulations at length scales comparable to the system size. These modulations appear to be qualitatively similar to transverse amplitude-type modulations seen in single-frequency patterns [9].

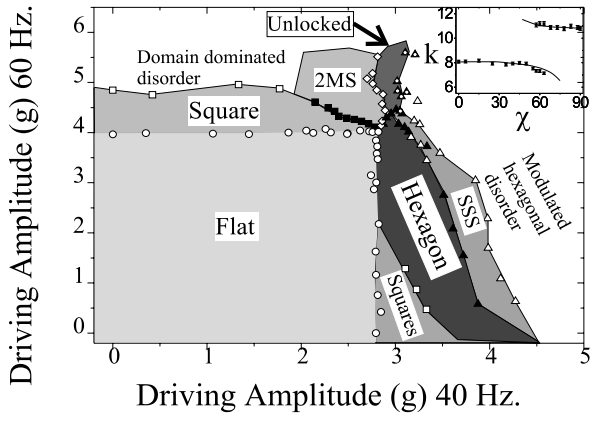

FIG. 1. A typical two-frequency phase diagram (obtained for $\omega_1/\omega_2 = 40/60$ Hz). Together with square and hexagonal phases, we observe three new states, SSS, 2MS, and spatially and temporally unlocked states (unlocked states). Symbols describe transition lines measured for fixed χ. A thin 2MS transition region (dotted triangles) to hexagons is also seen. (inset) A comparison of k (in cm^{-1}), calculated using the two-frequency linear calculation (line) [2], with measured values as a function of χ (in degrees).

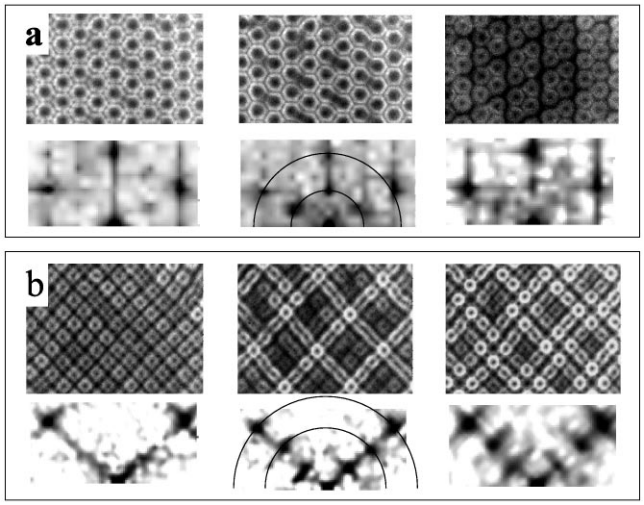

FIG. 2. Typical sequences of the SSS (a) and 2MS (b) superlattice states taken at constant values of the driving parameters for the frequency ratio 40/60 Hz. The SSS spatial Fourier spectra are composed solely of wave numbers $k1$, corresponding to $\omega_1/2$, and $k_1/2$, while the 2MS spectra are composed of *both* k_1 and k_2. In both states the *locations* of the peaks are fixed. Semicircles of radii k_1 and $k_1/2$ are drawn in (a) and k_1 and k_2 in (b).

Two-mode superlattices generally occur in regions of phase space where the higher frequency, ω_2, is dominant. As for SSS states, the transition to 2MS is nonhysteretic and occurs via propagating fronts. As Fig. 2b indicates, 2MS are qualitatively different than SSS as they result from spatial phase locking of *both* k_1 and k_2. The values of k_1 and k_2 measured throughout the phase diagram states are within 1%–2% of the values predicted by the two-frequency numerical code of Tuckerman [10] (see the inset in Fig. 1). These values are significantly different than the values of k excited by single-frequency excitation. The 2MS states are periodic in time with a basic frequency of ω_0 or $\omega_0/2$ for, respectively, odd-odd or odd-even values of n and m in Eq. (1). Thus, these states inherit the basic periodicity of both of the underlying primary bifurcations. Like the SSS, the state's appearance changes qualitatively with time with the spatial wave numbers having fixed *locations* and time-dependent *amplitudes*.

Although the two driving frequencies determine the lengths of k_1 and k_2, their relative orientations are governed by nonlinear interactions between them. 2MS spectra, as shown in Fig. 3, are composed of peaks of length k_1 and k_2 and their linear combinations. The strongest secondary peaks are given by $\vec{k}_3 = \vec{k}_2 - \vec{k}_1$, where the value of k_3 is consistent with the linear value of k calculated for a single-frequency excitation [11] at the difference frequency $\omega_3 = \omega_2 - \omega_1$. This suggests that the orientation of the wave vectors building the 2MS is selected by nonlinear interactions that are resonant both in space and time. Three-wave resonant interactions have been predicted to occur in nonlinear interactions of surface waves [12] and are well known in the physics of plasmas. States similar to 2MS have also been observed when an optical beam passes through a nonlinear medium [13]. The existence of this resonance condition is nontrivial, since the temporal resonance condition precisely determines the relative orientation of k_1 and k_2. Unlike, for example, the higher harmonics of k_1 and k_2 observed in the spectrum, the selection of k_3 via the temporal resonance condition yielding ω_3 cannot be accounted for by experimental artifacts such as possible nonlinearities in the imaging. We have observed this three-wave resonance condition for all frequency ratios tested. As in SSS, the dominant 2MS wave vector retains its initial symmetry, while the basic symmetry of the other excited wave vector state is broken with its relative orientations determined by the above resonance condition. Examples are shown in Fig. 3 where the dominant wave vectors are k_2 in (a) and (b) and k_1 in (c). These have, respectively, square, hexagonal, and hexagonal symmetries, which are retained. The basic symmetry of the nondominant wave vector, k_1 in (a) and (b) and k_2 in (c), is broken. Unlike the SSS states, when the amplitude of the driving is increased, the 2MS lose stability by the formation of uncorrelated domains in a way similar to the optical patterns observed in [13]. This suggests that instability of the state occurs when the spatial correlation length becomes smaller than the system size.

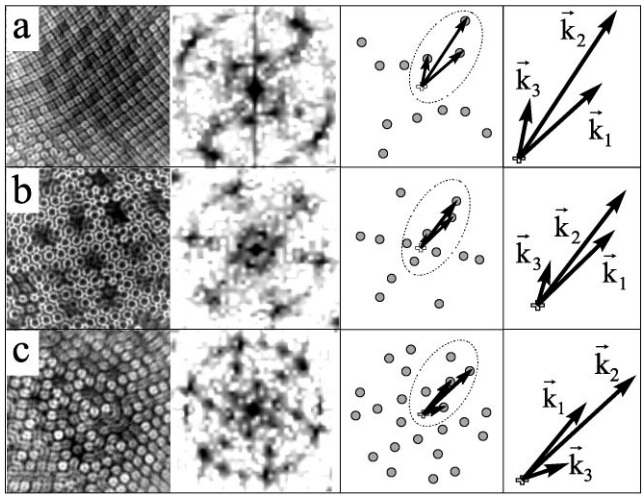

FIG. 3. Although ω_1 and ω_2 determine the length of k_1 and k_2, in 2MS, their relative orientations are determined by the condition: $\vec{k}_3 = \vec{k}_2 - \vec{k}_1$ where the length of k_3 is determined by the temporal resonance condition: $\omega_3 = \omega_2 - \omega_1$. 2MS patterns for (a) 50/80, (b) 45/60 (left of unlocked region), and (c) 40/60 Hz (dotted triangles in Fig. 1) are shown together with the triads, $\vec{k}_3 = \vec{k}_2 - \vec{k}_1$, observed in their respective spectra.

Let us now turn to the unlocked state that appears around the region of bistability of k_1 and k_2. In Fig. 4a we present typical photographs of an unlocked state with its corresponding spatial spectrum. The spatial behavior of the state varies rapidly in time. In contrast to the SSS and 2MS states, in the unlocked state no orientational order is apparent. Although, as in 2MS states, both k_1 and k_2 exist simultaneously in the spectrum, neither spatial nor temporal mode locking occurs. This is apparent in their power spectra, where, generally, entire circles of radii k_1 and k_2 are observed. Is the unlocked state a well-defined region of phase space or simply a narrow transition regime between 2MS and hexagonal phases? To address this question, we define, as in [14], the following "orientational correlation function" for a given value of k:

$$C_k(\theta) \equiv \Sigma_\alpha[f_k(\alpha)f_k(\alpha + \theta)]/\Sigma_\alpha[f_k(\alpha)f_k(\alpha)], \quad (2)$$

where $f_k(\alpha)$ is the Fourier transform of the wave number k at the polar angle θ. As both the 2MS and hexagonal states have clear orientational order, $C_k(\theta)$ is a sensitive probe of the unlocked regime, providing information about the type and degree of orientational symmetry within a given state. We quantify the degree of orientational order in a given pattern by means of the *orientational amplitude*, $Q_k = 1/2[\max C_k(\theta) - \min C_k(\theta)]$, which varies between 0 and 1 for, respectively, minimal and maximal orientational order. In Fig. 4 we present mean values of Q_k, over a single period, for both k_1 and k_2 along the line $\chi = 58°$, which

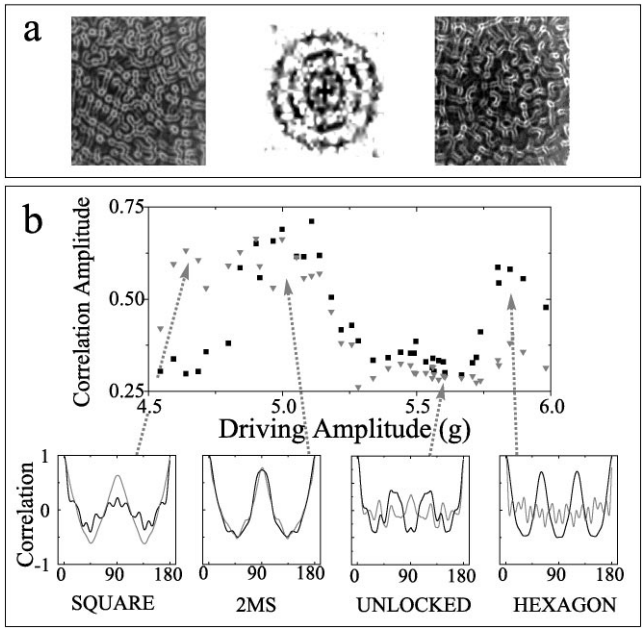

FIG. 4. In the unlocked state no orientational order is apparent. As in 2MS states, k_1 and k_2 exist simultaneously, but unlocked state spectra are diffuse and show little angular correlation. (a) (left–right) Typical views of an unlocked state observed for 40/60 Hz driving at different times. The spectrum (center) corresponds to the pattern on the left. Throughout the unlocked phase the correlation amplitude, Q_k drops significantly although the angular correlation function, $C_k(\theta)$, indicates a small amount of residual order. (b) (upper) Q_{k_1} (triangles) and Q_{k_2} (squares), averaged over a single period along the line $\chi = 58°$ for 40/60 Hz driving as a function of the driving amplitude, A. This line traverses the square, 2MS, unlocked, and hexagonal phases. The symmetry of the different phases is highlighted by $C_k(\theta)$, for k_1 (grey line) and k_2 (black line) computed for typical states (θ is in degrees). The power (log scale) of k_2 relative to k_1 in each $C_k(\theta)$ is 8.3 (square), 1.1 (2MS), 0.9 (unlocked), and 0.2 (hexagon).

passes through the square, 2MS, unlocked, and hexagonal phases.

As apparent from Fig. 4a, the orientational amplitude drops sharply as the boundary between the 2MS and unlocked phases is crossed. Surprisingly, however, the representative $C_k(\theta)$ plots in Fig. 4 indicate a small amount of residual order in the latter phase. A transition from the square symmetry, which dominates both k_1 and k_2 in the 2MS state, to a small degree of mixed square and hexagonal order within the unlocked state is evident. After the transition to the unlocked phase, Q_k remains at the same level until reaching the hexagonal phase boundary. At this point Q_k increases significantly, and pure hexagonal symmetry is observed in the corresponding $C_k(\theta)$. Thus, we see that the unlocked phase corresponds to a broad, well-defined region of phase space that is characterized by a lack of orientational order.

In conclusion, in the above experiments we have begun to address the basic question of what types of states are selected by a dissipative nonlinear system when nonlinear waves having two different basic wavelengths, but infinite degeneracy, are simultaneously excited. We find that, as the relative "weights" of the waves are varied via their excitation amplitudes, three qualitatively different types of multiwave states arise as either primary or secondary bifurcations. These states are qualitatively similar to states observed in both nonlinear optics [13] and recent simulations [6]. These states exhibit interesting spatial and temporal behavior not observed in systems in which only a single basic mode is excited. It remains to be seen whether the routes to spatial and temporal complexity, observed in this particular system, are taken by additional driven dissipative systems.

The authors acknowledge the support of the Israel Academy of Science Grants No. 43/93-2 and No. 9050/93. We thank L. S. Tuckerman for the use of her linear stability code.

[1] (a) W. S. Edwards and S. Fauve, Phys. Rev. E **47**, 788 (1993); (b) J. Fluid Mech. **278**, 123 (1994).
[2] T. Besson, W. S. Edwards, and L. S. Tuckerman, Phys. Rev. E **54**, 507 (1996).
[3] K. Kumar and L. S. Tuckerman, J. Fluid Mech. **279**, 49 (1994).
[4] H. W. Muller, H. Wittmer, C. Wagner, J. Albers, and K. Knorr, Phys. Rev. Lett. **78**, 2357 (1997).
[5] W. Zhang and J. Vinals, J. Fluid Mech. **341**, 225 (1997).
[6] R. Lifshitz and D. M. Petrich, Phys. Rev. Lett. **79**, 1261 (1997).
[7] O. Lioubashevski, H. Arbell, and J. Fineberg, Phys. Rev. Lett. **76**, 3959 (1996).
[8] Similar states, for two-frequency forcing, have been observed in other parameter regimes by J. P. Gollub (private communication).
[9] L. Daudet, V. Ego, S. Manneville, and J. Bechhoefer, Europhys. Lett. **32**, 313 (1995); A. Kudrolli and J. P. Gollub, Physica (Amsterdam) **97D**, 133 (1996).
[10] k was calculated with the code used in [3].
[11] The calculated value of k_3 is obtained using the *linear* single-frequency code of [3] at threshold. The difference between the calculated and measured values varies between 5%–20%, but this shift in k is constant for a given value of the difference frequency, ω_3, and systematically decreases as ω_3 increases. This shift may be the result of either finite size effects in the cell or the nonlinear coupling of k_1 and k_2.
[12] See, e.g., J. L. Hammack, Annu. Rev. Fluid Mech. **25**, 55 (1993).
[13] E. Pampaloni, S. Residori, S. Soria, and F. T. Arecchi, Phys. Rev. Lett. **78**, 1042 (1997).
[14] D. Binks and W. van de Water, Phys. Rev. Lett. **78**, 4043 (1997).